Improved Active Power Filter Performance for Renewable Power Generation Systems by Using Fuzzy Logic Controller

S. Naga Purnima[1], N. Dharani Kumar[2]

PG Student, Dept. of EEE, RVR&JC College of Engineering, Chowdavaram, Guntur, AP, India[1]

Assistant Professor, Dept. of EEE, RVR&JC College of Engineering, Chowdavaram, Guntur, AP, India[2]

ABSTRACT: In this paper active power filter implementation with four leg VSC using a fuzzy logic controller scheme is presented. By using the four leg voltage source converter allows the compensation of current harmonic components as well as unbalanced current generated by non liner loads . the compensation performance of the proposed active power filter and transient operating conditions. In recent times fuzzy logic controller was applied for active power filter controller applications. In this paper A Fuzzy logic based shunt active power filter is presented and verified in Matlab simulation software.

KEYWORDS: Active power filter, current controller, four leg converters, fuzzy logic controller.

I. INTRODUCTION

Renewable generation affects power quality due to its nonlinearity, since solar generation plants and wind power generators must be connected to the grid through high-power static PWM converters [2]. The non uniform nature of power generation directly affects voltage regulation and creates voltage distortion in power systems. This new scenario in power distribution systems will require more sophisticated compensation techniques. Although active power filters implemented with three-phase four-leg voltage-source inverters (4L-VSI) have already been presented in the technical literature [3]– [7], the primary contribution of this paper is a predictive control algorithm designed and implemented specifically for this application. Traditionally, active power filters have been controlled using fuzzy logic controller.

An accurate model obtained using fuzzy logic controllers improves the performance of the active power filter, especially during transient operating conditions, because it can quickly follow the current-reference signal while maintaining a constant dc-voltage. So far, implementations of fuzzy logic control in power converters have been used mainly in induction motor drives[10]–[17].In the case of motor drive applications, fuzzy logic control represents a very intuitive control scheme that handles multivariable characteristics, simplifies the treatment of dead-time compensations, and permits pulse-width modulator replacement. However, these kinds of applications present disadvantages related to oscillations and instability created from unknown load parameters [16]. One advantage of the proposed algorithm is that it fits well in active power filter applications, since the power converter output parameters are well known [18].

These output parameters are obtained from the converter output ripple filter and the power system equivalent impedance. The converter output ripple filter is part of the active power filter design and the power system impedance is obtained from well-known standard procedures [19], [20].In the case of unknown system impedance parameters, an estimation method can be used to derive an accurate $R–L$ equivalent impedance model of the system [21].

This paper presents the mathematical model of the 4L-VSI and the principles of operation of the proposed predictive control scheme, including the design procedure. The complete description of the selected current reference generator implemented in the active power filter is also presented. Finally, the proposed active power filter and the effectiveness of the associated control scheme compensation are demonstrated through simulation results are obtained.

II. FOUR-LEG CONVERTER MODEL

The below Fig. 1 shows the configuration of a typical power distribution system with renewable power generation. It consists of various types of power generation units and different types of loads. Renewable sources, such as wind and sunlight, are typically used to generate electricity for residential users and small industries. Both types of power generation use ac/ac and dc/ac static PWM converters for voltage conversion and battery banks for long term energy storage. These converters perform maximum power point tracking to extract the maximum energy possible from wind and sun. The electrical energy consumption behavior is random and unpredictable, and therefore, it may be single- or three-phase, balanced or unbalanced, and linear or nonlinear. An active power filter is connected in parallel at the point of common coupling to compensate current harmonics, current unbalance, and reactive power. It is composed by an electrolytic capacitor, a four-leg PWM converter, and a first order output ripple filter, as shown in Fig. 2. This circuit considers the power system equivalent impedance Zs, the converter output ripple filter impedance Zf, and the load impedance ZL.
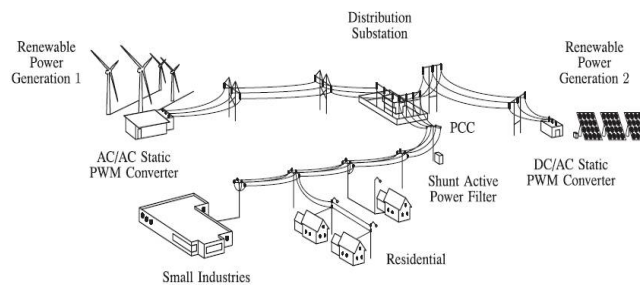

Fig 1. Stand-alone hybrid power generation system with a shunt active power filter.

The four-leg PWM converter topology is shown in Fig. 3. This converter topology is similar to the conventional three-phase converter with the fourth leg connected to the neutral bus of the system. The fourth leg increases switching states from 8 (23) to 16 (24),improving control flexibility and output voltage quality [21], and is suitable for current unbalanced compensation.
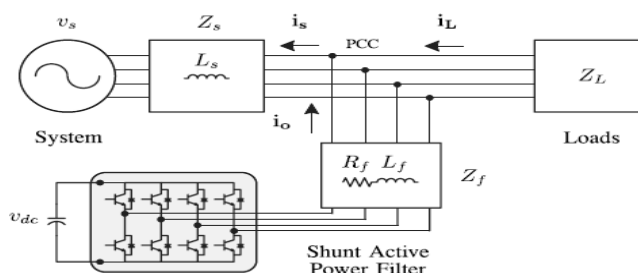

Fig 2 Three-phase equivalent circuit of the proposed shunt active power filter.
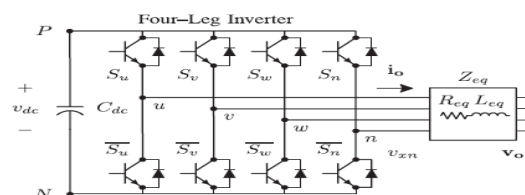

Fig 3 Two-level four-leg PWM-VSI topology

The voltage in any legx of the converter, measured from the neutral point (n), can be expressed in terms of switching states, as follows:

$$v_{xn} = S_x - S_n v_{dc}, \quad x = u, v, w, n. \qquad (1)$$

The mathematical model of the filter derived from the equivalent circuit shown in Fig. 2 is

$$V_0 = v_{xn} - R_{eq}i_0 - L_{eq}\frac{di_0}{dt} \qquad (2)$$

Where Req and Leq are the 4L-VSI output parameters expressed as Thevenin impedances at the converter output terminals Zeq. Therefore, the Thevenin equivalent impedance is determined by a series connection of the ripple filter impedance Zf and a parallel arrangement between the system equivalent impedance Zs and the load impedance

$$Z_{eq} = \frac{Z_s Z_L}{Z_s + Z_L} + Z_f \approx Z_s + Z_f \qquad (3)$$

ZL

For this model, it is assumed that $Z_L \gg Z_s$, that the resistive part of the system's equivalent impedance is neglected, and that the series reactance is in the range of 3–7% p.u., which is an acceptable approximation of the real system. Finally, in (2) Req =Rf and Leq =Ls+Lf.

III. DIGITALPREDICTIVECURRENTCONTROL

The block diagram of the proposed digital predictive current control scheme is shown in Fig. 3.4. This control scheme is basically an optimization algorithm and, therefore, it has to be implemented in a microprocessor. Consequently, the analysis has to be developed using discrete mathematics in order to consider additional restrictions such as time delays and approximations
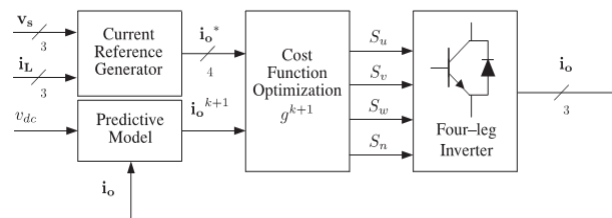

Fig. 4. Proposed predictive digital current control block diagram

[10], [22]–[27]. The main characteristic of predictive control is the use of the system model to predict the future behaviour of the variables to be controlled. The controller uses this information to select the optimum switching state that will be applied to the power converter, according to predefined optimization criteria. The predictive control algorithm is easy to implement and to understand, and it can be implemented with three main blocks, as shown in Fig. 4.

A. Current Reference Generator:
This unit is designed to generate the required current reference that is used to compensate the undesirable load current components. In this case, the system voltages, the load currents, and the dc-voltage converter are measured, while the neutral output current and neutral load current are generated directly from these signals (IV).

B. Prediction Model:
The converter model is used to predict the output converter current. Since the controller operates indiscrete time, both the controller and the system model must be represented in a discrete time domain [22]. The discrete time model consists of a recursive matrix equation that represents this prediction system. This means that for a given sampling time Ts, knowing the converter switching states and control variables at Instant kTs, it is possible to predict the next states at any instant [k+1]Ts. Due to the first-order nature of the state equations that describe the model in (1)–(2), a sufficiently accurate first-order approximation of the derivative is considered in this paper

$$\frac{dx}{dt} \approx \frac{x[k+1]-x[k]}{T_S} \qquad (4)$$

The 16 possible output current predicted values can be obtained from (2) and (4) as

$$i_0[k+1] = \frac{T_S}{L_{eq}}(v_{xn}[k]-V_0[k])+\left(1-\frac{R_{eq}}{L_{eq}}\right)i_0[k]. \tag{5}$$

As shown in (5), in order to predict the output current i_o at the instant (k+1), the input voltage value v_o and the converter output voltage v_{xn}, are required. The algorithm calculates all 16 values associated with the possible combinations that the state variables can achieve.

C. Cost Function Optimization:

In order to select the optimal switching state that must be applied to the power converter, the 16 predicted values obtained for $i_o[k+1]$ are compared with the reference using a cost function, as follows:

$$g[k+1]=(i_{ou}^*[k+1]-i_{ou}[k+1])2+(i_{ov}^*[k+1]-i_{ov}[k+1])^2+(i_{ow}^*[k+1]-i_{ow}[k+1])^2+(i_{on}^*[k+1]-i_{on}[k+1])^2 \tag{6}$$

The output current (i_o) is equal to the reference (i^*_o) when g=0. Therefore, the optimization goal of the cost function is to achieve a g value close to zero. The voltage vector v_{xN} that minimizes the cost function is chosen and then applied at the next sampling state. During each sampling state, the switching state that generates the minimum value of g is selected from the 16 possible function values. The algorithm selects the switching state that produces this minimal value and applies it to the converter during the k+1 state.

D. Current Reference Generation

A dq-based current reference generator scheme is used to obtain the active power filter current reference signals. This scheme presents a fast and accurate signal tracking capability. This characteristic avoids voltage fluctuations that deteriorate the current reference signal affecting compensation performance [28]. The current reference signals are obtained from the corresponding load currents as shown in Fig. 3.5. This module calculates the reference signal currents required by the converter to compensate reactive power, current harmonic and current imbalance. The displacement power factor ($\sin\varphi$ (L)) and the maximum total harmonic distortion of the load (THD (L)) defines the relationships between the apparent power required by the active power filter, with respect to the load, as shown

$$\frac{S_{APF}}{S_L} = \frac{\sqrt{sin\emptyset_L + THD_{(L)}^2}}{\sqrt{1 + THD_{(L)}^2}} \tag{7}$$

Where the value of THD (L) includes the maximum compensable harmonic current, defined as double the sampling frequency f_s. The frequency of the maximum current harmonic component that can be compensated is equal to one half of the converter switching frequency. The dq-based scheme operates in a rotating reference frame. Therefore, the measured currents must be multiplied by the sin(wt) and cos(wt) signals. By using dq-transformation, the d current component is synchronized with the corresponding phase-to-neutral system voltage, and the q current component is phase-shifted by 90°. The sin(wt) and cos(wt) synchronized reference signals are obtained from a synchronous reference frame (SRF) PLL [29]. The SRF-PLL generates a pure sinusoidal waveform even when the system voltage is severely
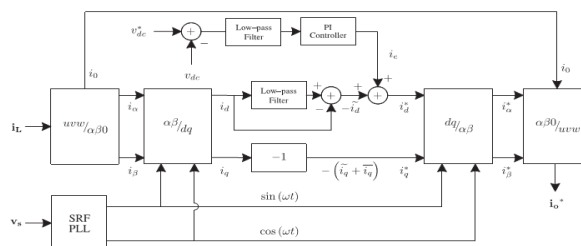

Fig. 5. Dq-based current reference generator block diagram.

Distorted. Tracking errors are eliminated, since SRF-PLLs are designed to avoid phase voltage unbalancing, harmonics (i.e.,less than 5% and 3% in fifth and seventh, respectively), and offset caused by the nonlinear load conditions and measurement errors [30]. Equation (8) shows the relationship between the real currents iLx(t)(x=u, v, w) and the associated dq components(id and iq)

$$\begin{bmatrix} i_d \\ i_q \end{bmatrix} = \sqrt{\frac{2}{3}} \begin{bmatrix} \sin \omega t & \cos \omega t \\ -\cos \omega t & \sin \omega t \end{bmatrix} \begin{bmatrix} 1 & -1/2 & -1/2 \\ 0 & \sqrt{3}/2 & -\sqrt{3}/2 \end{bmatrix} \begin{bmatrix} i_{Lu} \\ i_{Lv} \\ i_{Lw} \end{bmatrix} \quad (8)$$

A low-pass filter (LFP) extracts the dc component of the phase currents id to generate the harmonic reference components− i_d. The reactive reference components of the phase-currents are obtained by phase-shifting the corresponding ac and dc components of i_q by 180∘. In order to keep the dc-voltage constant, the amplitude of the converter reference current must be modified by adding an active power reference signal ie with the d-component, as will be explained in Section IV-A. The resulting signals i^*_d and i^*_q are transformed back to a three-phasesystem by applying the inverse Park and Clark transformation,as shown in (9). The cutoff frequency of the LPF used in thispaper is 20 Hz

$$\begin{bmatrix} i^*_{ou} \\ i^*_{ov} \\ i^*_{ow} \end{bmatrix} = \sqrt{\frac{2}{3}} \begin{bmatrix} \frac{1}{2} & 1 & 0 \\ \frac{1}{\sqrt{2}} & -\frac{1}{2} & \frac{\sqrt{3}}{2} \\ \frac{1}{\sqrt{2}} & -\frac{1}{2} & -\frac{\sqrt{3}}{2} \end{bmatrix} \begin{bmatrix} 1 & 0 & 0 \\ 0 & \sin \omega t & -\cos \omega t \\ 0 & \cos \omega t & \sin \omega t \end{bmatrix} \begin{bmatrix} i_o \\ i^*_d \\ i^*_q \end{bmatrix} \quad (9)$$

The current that flows through the neutral of the load is compensated by injecting the same instantaneous value obtained From the phase-currents, phase-shifted by 180∘, as shown next

$$i^*_{on} = -(i_{Lu} + i_{Lv} + i_{Lv}) \quad (10)$$

One of the major advantages of the dq-based current reference generator scheme is that it allows the implementation of a linear controller in the dc-voltage control loop. However, one important disadvantage of the dq-based current reference frame algorithm used to generate the current reference is that a second order harmonic component is generated in id and iq under unbalanced operating conditions. The amplitude of this harmonic depends on the percent of unbalanced load current (expressed as the relationship between the negative sequence current i_{L2}andthe positive sequence current i_{L1}). The second-order harmonic cannot be removed from i_d and i_q, and therefore generates 3.athird harmonic in the reference current when it is converted back to abc frame [31]. Fig. 3.6 shows the percent of system current imbalance and the percent of third harmonic system current, in function of the percent of load current imbalance. Since the load current does not have a third harmonic, the one generated by the active power filter flows to the power system.
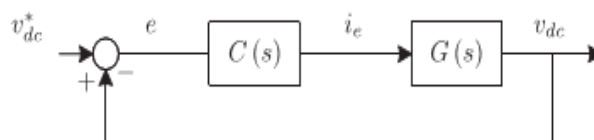

Fig. 6. DC-voltage control block diagram.

IV. DC-VOLTAGE CONTROL

The dc-voltage converter is controlled with a traditional PI controller. This is an important issue in the evaluation, since the cost function (6) is designed using only current references, in order to avoid the use of weighting factors. Generally, these weighting factors are obtained experimentally, and they are not well defined when different

operating conditions are required. Additionally, the slow dynamic response of the voltage across the electrolytic capacitor does not affect the current transient response. For this reason, the PI controller represents a simple and effective alternative for the dc-voltage control. The dc-voltage remains constant (with a minimum value of $\sqrt{6}v_s$(RMS)) until the active power absorbed by the converter decreases to a level where it is unable to compensate for its losses. The active power absorbed by the converter is controlled by adjusting the amplitude of the active power reference signal ie, which is in phase with each phase voltage. In the block diagram shown in Fig. 3.5, the dc-voltage v_{dc} is measured and then compared with a constant reference value v^*_{dc}. The error(e) is processed by a PI controller, with two gains, Kp and Ti. Both gains are calculated according to the dynamic response requirement. Fig. 6 shows that the output of the PI controller is fed to the dc-voltage transfer function Gs, which is represented by a first-order

$$G(s) = \frac{v_{dc}}{i_c} = \frac{3}{2} \frac{K_p v_s \sqrt{2}}{C_{dc} v^*_{dc}} \qquad (11)$$

The equivalent closed-loop transfer function of the given system with a PI controller (12) is shown in (13)

$$C(s) = K_p(1 + \frac{1}{T_i.s}) \qquad (12)$$

$$\frac{v_{dc}}{i_c} = \frac{\frac{w^2_n}{a}.(s+a)}{s^2 + 2(w_n.s + w^2_n)} \qquad (13)$$

Since the time response of the dc-voltage control loop does not need to be fast, a damping factor $\zeta=1$ and a natural angular speed $\omega n=2\pi\cdot100$ rad/s are used to obtain a critically damped response with minimal voltage oscillation. The corresponding integral time Ti =1/a(13) and proportional gain Kp can be calculated as

$$\delta = \sqrt{\frac{3}{8} \frac{K_p v_s \sqrt{2 T_i}}{C_{dc} v^*_{dc}}} \qquad (14)$$

$$\omega_n = \sqrt{\frac{3}{2} \frac{K_p v_s \sqrt{2}}{C_{dc} v^*_{dc} T_i}} \qquad (15)$$

V. FUZZY LOGIC CONTROLLER

In FLC, basic control action is determined by a set of linguistic rules. These rules are determined by the system. Since the numerical variables are converted into linguistic variables, mathematical modeling of the system is not required in FC. The FLC comprises of three parts: Fuzzification , interference engine and defuzzification. The FC is characterized as

i. seven fuzzy sets for each input and output ,ii. Triangular membership functions for simplicity, iii. Fuzzification using continuous universe of discourse, iv. Implication using Mamdani's, 'min' operator. v. Defuzzification using the height method.

A. Fuzzification: Membership function values are assigned to the linguistic variables, using seven fuzzy subsets: NB (Negative Big), NM (Negative Medium), NS (Negative Small), ZE (Zero), PS (Positive Small),
PM (Positive Medium), and PB (Positive Big).
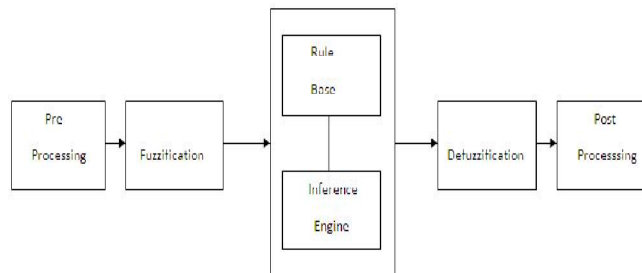
Fig 7 Fuzzy logic controller

B. Table I Fuzzy Rules

Change in error	Error						
	NB	NM	NS	Z	PS	PM	PB
NB	PB	PB	PB	PM	PM	PS	Z
NM	PB	PB	PM	PM	PS	Z	Z
NS	PB	PM	PS	PS	Z	NM	NB
Z	PB	PM	PS	Z	NS	NM	NB
PS	PM	PS	Z	NS	NM	NB	NB
PM	PS	Z	NS	NM	NM	NB	NB
PB	Z	NS	NM	NM	NB	NB	NB
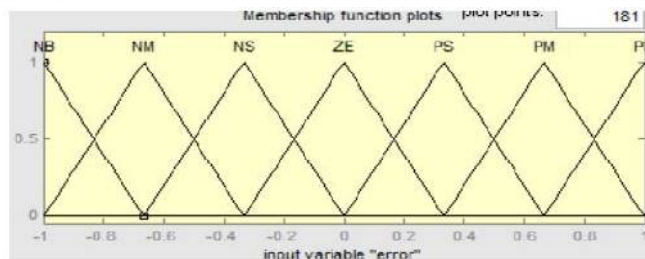
Fig 8 Membership functions

B. Inference Method: Several composition methods such as Max–Min and Max-Dot have been proposed in the literature. In this paper Min method is used. The output membership function of each rule is given by the minimum operator and maximum operator. Table 1 shows rule base of the FLC.

C. Defuzzification: As a plant usually requires a non fuzzy value of control, a defuzzification stage is needed. To compute the output of the FLC, „height" method is used and the FLC output modifies the control output. Further, the output of FLC controls the switch in the inverter. In UPQC, the active power, reactive power, terminal voltage of the line and capacitor voltage are required to be maintained. In order to control these parameters, they are sensed and compared with the reference values. To achieve this, the membership functions of FC are: error, change in error and output

VI. SIMULATED RESULTS
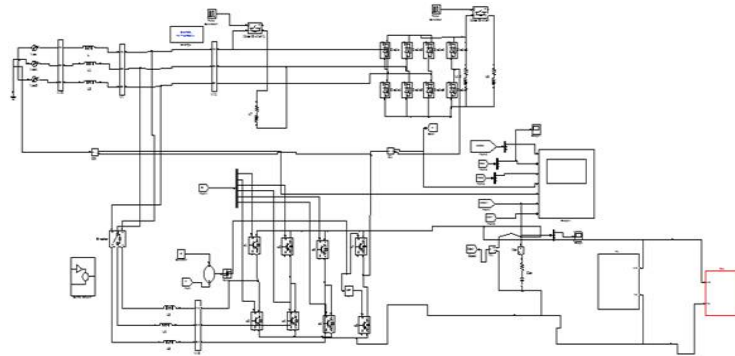
Fig9 Circuit Diagram of Active Power Filter Using Hybrid Fuzzy Controller For RES
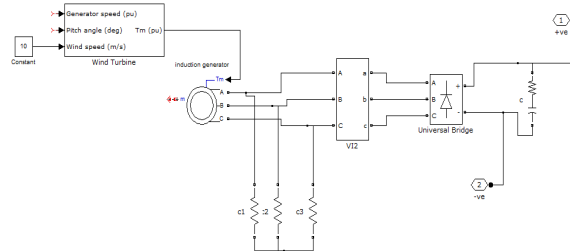
Fig 10 wind Power Generation System
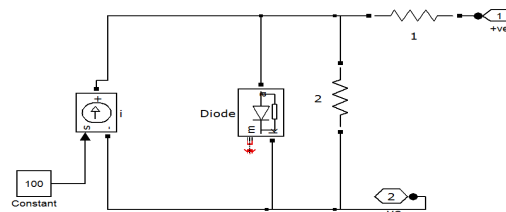

Fig 11 solar power generation system
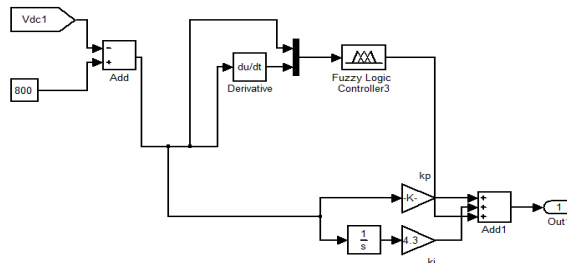

Fig 12 Hybrid Fuzzy Controller
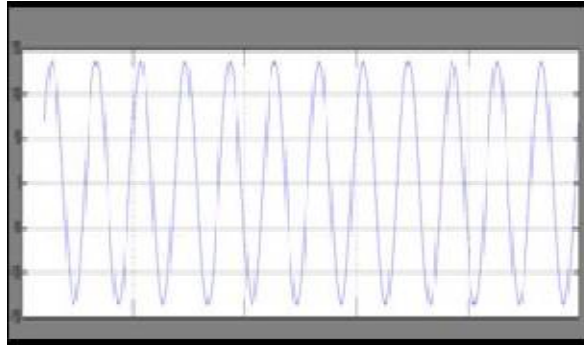
Fig 13 Phase to neutral source voltage
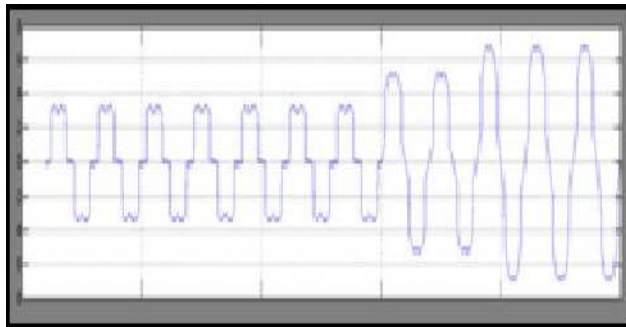
Fig 14 Load Current.
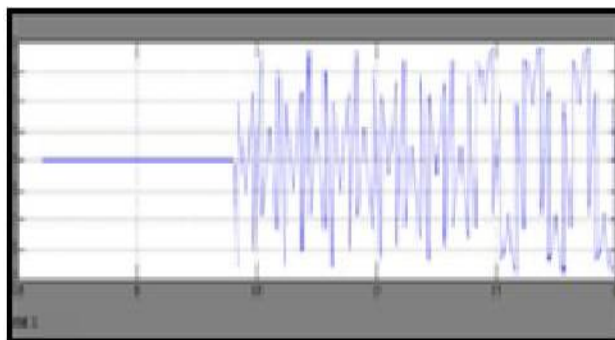
Fig15 Active power filter output current.
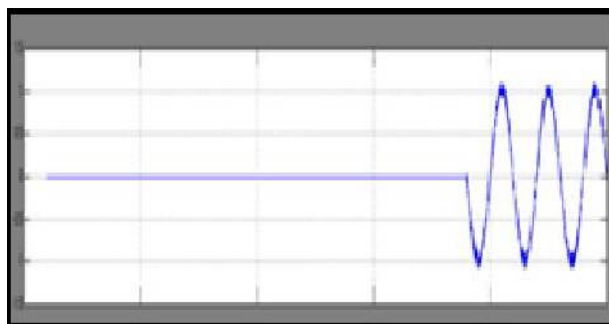
Fig16 Load neutral current
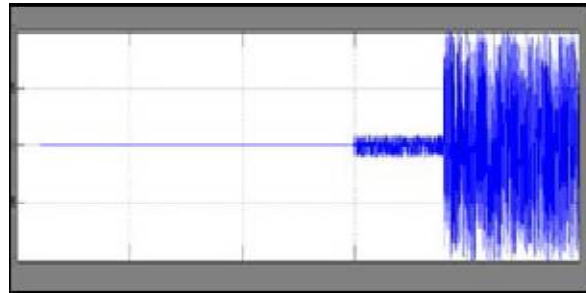
Fig 17 System neutral current.
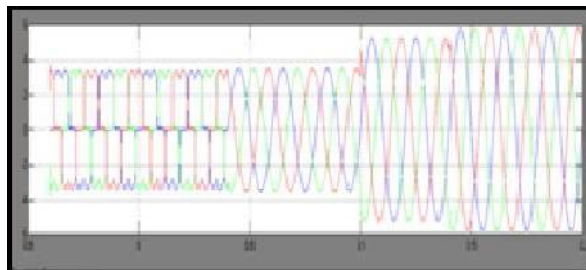
Fig 18 System currents.
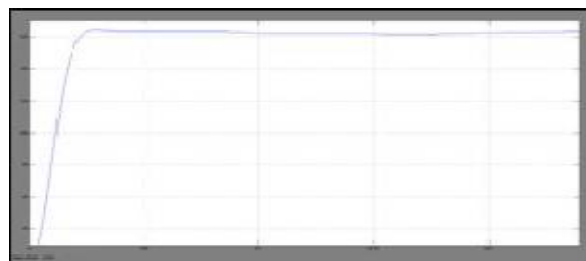

Fig 19 DC voltage converter.
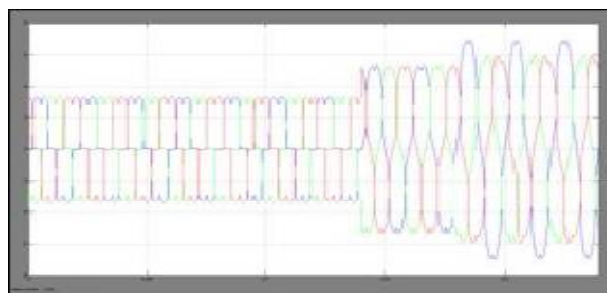
Fig 20 Non linear load current

VII. CONCLUSION

Improved dynamic current harmonics and a reactive power compensation scheme for power distribution systems with generation from renewable sources has been proposed to improve the current quality of the distribution system. Advantages of the proposed scheme are related to its simplicity, modeling, and implementation. Simulated results have proved that the proposed predictive control algorithm is a good alternative to classical linear control methods. The predictive current control algorithm is a stable and robust solution. Simulated results have shown the compensation effectiveness of the proposed active power filter.

In this paper, The use of fuzzy logic controller proved to be an effective solution for active power filter applications. It will improves the current tracking capability, Dynamic performance and transient response. Simulated results have proved that the proposed fuzzy control method is good alternative to renewable power generation systems. An improved fuzzy logic based shunt APF is proposed, which is suitable for digital control realization.

REFERENCES

[1] Pablo Acuna,Luis Moran,Marco Rivera,Juan Dixon, and Jos Rodriguez, "Improved active power filter performance for renewable powe generation systems," *IEEE Trans. Power Electron.*, vol. 29, no. 2, pp. 0885-8993, Feb. 2014.

[2] J. Rocabert, A. Luna, F. Blaabjerg, and P. Rodriguez, "Control of power converters in AC microgrids," *IEEE Trans. Power Electron.*, vol. 27, no. 11, pp. 4734–4749, Nov. 2012.

[3] M. Aredes, J. Hafner, and K. Heumann, "Threephase four-wire shunt active filter control strategies," *IEEE Trans. Power Electron.*, vol. 12, no. 2, pp. 311– 318, Mar. 1997.

[4] S. Naidu and D. Fernandes, "Dynamic voltage restorer based on a fourleg voltage source converter,"
Gener. Transm. Distrib., IET, vol. 3, no. 5, pp. 437–447, May 2009.

[5] N. Prabhakar and M. Mishra, "Dynamic hysteresis current control to minimize switching for three-phase four-leg VSI topology to compensate nonlinear load," *IEEE Trans. Power Electron.*, vol. 25, no. 8, pp. 1935–1942, Aug. 2010.

[6] V. Khadkikar, A. Chandra, and B. Singh, "Digital signal processor implementation and performance evaluation of split capacitor, four-leg and three h-bridge-based three-phase four-wire shunt active filters," *Power Electron., IET*, vol. 4, no. 4, pp. 463–470, Apr. 2011.

[7] F. Wang, J. Duarte, and M. Hendrix, "Gridinterfacing converter systems with enhanced voltage quality for micro grid application; concept and implementation," *IEEE Trans. Power Electron.*, vol. 26, no. 12, pp. 3501– 3513, Dec. 2011

[8] X. Wei, "Study on digital pi control of current loop in active power filter,"in *Proc. 2010 Int. Conf.*
Electr. Control Eng., Jun. 2010, pp. 4287–4290.

[9] R. de Araujo Ribeiro, C. de Azevedo, and R. de Sousa, "A robust adaptive control strategy of active
power filters for power-factor correction, harmonic compensation, and balancing of nonlinear loads," *IEEE Trans. Power Electron.*, vol. 27, no. 2, pp. 718–730, Feb. 2012.

[10] J. Rodriguez, J. Pontt, C. Silva, P. Correa, P. Lezana, P. Cortes, and U. Ammann, "Predictive current control of a voltage source inverter," *IEEE Trans. Ind. Electron.*, vol. 54, no. 1, pp. 495– 503, Feb. 2007.